

The Effect of Al-Cu Co-Dopants on Morphology, Structure, and Optical Properties of ZnO Nanostructures

I. Sugihartono^{a*} , S.T. Tan^b, A. Arkundato^c, R. Fahdiran^a, I. Isnaeni^d, E. Handoko^a, S. Budi^e, A.S. Budi^e

^aUniversitas Negeri Jakarta, Program Studi Fisika FMIPA, Jalan Rawamangun Muka no. 01, 13220, Jakarta Timur, Indonesia.

^bXiamen University Malaysia, School of Energy and Chemical Engineering, 43900, Selangor Darul Ehsan, Malaysia.

^cUniversitas Jember, Program Studi Fisika FMIPA, Jalan Kalimantan, Jember, 68121, Jawa Timur, Indonesia.

^dIndonesian Institute of Sciences, Research Center for Physics, 15314, Banten, Indonesia.

^eUniversitas Negeri Jakarta, Program Studi Kimia FMIPA, Jalan Rawamangun Muka no. 01, 13220, Jakarta Timur, Indonesia.

Received: November 24, 2022; Revised: March 08, 2023; Accepted: March 30, 2023

We have synthesized ZnO nanostructure by using two-step methods i.e ultrasonic nebulizer and chemical bath deposition (CBD) at 95°C for two hours. The morphology, structural, reflectance, and photoluminescence properties have been characterized by the scanning electron microscope (SEM), the X-ray diffraction (XRD) measurement, ultraviolet-visible (UV-Vis) spectrophotometer, and photoluminescence spectrometer, respectively. Structurally, all samples possess polycrystalline hexagonal wurtzite structure, and the addition of Al-Cu decreases the crystallinity of ZnO nanostructures. Meanwhile, morphologically, the role of Cu dopants in Al-Cu co-doped ZnO nanostructures suppressed the growth of nanostructures in the c-axis. Hence, it can be used to modify the morphology of ZnO nanorods to nanodisks/nanosheets. Optically, the Al-Cu co-dopants can be used to shift the optical band gap energy of ZnO nanostructures to a lower wavelength (blueshift). The photoluminescence (PL) properties confirmed that the Al-Cu co-dopants have two peaks at the photon energy of 3.78 eV and 3.90 eV.

Keywords: Al-Cu co-doped ZnO nanostructures, structure, morphology, optical band gap energy, photoluminescence.

1. Introduction

For the past two decades, as a hexagonal wurtzite structure, ZnO has been extensively studied. It is due to the large band gap energy of 3.34 eV, high exciton binding energy of 60 meV, broad optical absorption, high electron mobility, high transparency, and high photostability^{1,2}. Besides, ZnO is economically inexpensive, stable, has higher quantum efficiency, and natural abundance^{3,4}. Therefore, ZnO as II-VI semiconductor material is believed to have broad potential applications as optoelectronic devices.

As well known, ZnO as a multifunctional semiconductor material has been synthesized in a one-dimensional structure (i.e. nanorods, nanotubes, nanocombs, etc.) to improve its efficiency for use in many applications². The development of ZnO nanorods as a one-dimensional structure has been demonstrated by different methods, growth parameters, dopants, and annealing treatments^{1,3,5}. The different methods and growth parameters have been demonstrated in the preliminary study of ZnO nanorods. Meanwhile, various dopants are still become major interests to improve ZnO nanorods properties for some potential applications such as

solar cells (SCs)⁶, light emitting diodes (LEDs)⁷, sensors⁸, photocatalysts⁹, etc.

To the best of our knowledge, various metal ions such as Al, Mg, Co, Cu, etc have been used as dopants to change the electronic structure and other physical properties of ZnO nanorods^{4,10}. Among these metal ions, the Cu dopant in the ZnO lattice is used magnetic atoms. Besides, the presence of Cu in ZnO structure causes the substitution of Zn by Cu ions due to the size similarity of Cu (0.096 nm) and Zn (0.075 nm)⁴. Zhang et al.¹⁰ observed that Cu incorporation in ZnO structure causes bound exciton which is responsible for the enhancement of UV emission¹⁰. Another study reported that Cu partially replaced Zn ions. Then, it provides Cu-Zn complex defects that generate more electrons in the conduction band¹¹. Consequently, oxygen vacancies increased in the valence band. On the other hand, to improve the conductivity of Cu-doped ZnO nanorods, the Al elements have been chosen by Chakraborty et al.⁴ as a potential dopant candidate⁴. Others reported that in the presence of Al dopants in Cu-doped ZnO, the resistivity of the films decreased compared to Cu-doped ZnO¹². Bu et al.¹² believed that the electrical properties of Al-Cu co-doping ZnO nanorods can be tuned by the control Cu/Al ratio¹². Meanwhile, our previous results

*e-mail: iwan-sugihartono@unj.ac.id

indicated that Cu dopants suppressed the preferential growth of Al co-doped ZnO nanostructure along the *c*-axis¹. Then, morphologically the Al-Cu co-doped ZnO nanostructures changed to square nano-disk/nanosheets. On the other hand, Al ion is considered a dopant for ZnO nanostructures in terms of non-toxicity, high electron density, and the ability to decrease band gap energy¹³. The small size of Al with an ion radius of 0.053 nm is believed can substitute Zn easily and improve the crystallinity of ZnO⁶.

Annealing is an important treatment to improve the structural and other physical properties of ZnO nanostructure. By annealing at 500°C, Yang et al.¹⁴ confirmed that the crystallization and UV photoluminescence of ZnO nanorods enhanced¹⁴. A similar report was confirmed that the annealing temperature of 500°C caused recrystallization which observed from the (002) peak which shifted to a lower angle and has a significantly increasing intensity¹⁵. Others reported that with an annealing temperature of up to 800°C, the number of oxygen vacancies increased¹⁶. While Barnett et al.¹⁷ observed that annealing the ZnO nanorods at 800°C causes the hollow structure and the reduction of the depth emission¹⁷. Meanwhile, at the temperature of 500°C, the deep-level emission (DLE) peak shifted to the wavelength of 640nm. On the other hand, annealing in the atmosphere ambient can reduce the donor-related defects of ZnO¹⁸. It indicates that the annealing treatment at the proper temperature plays a significant role in modifying the structure and intrinsic defects responsible for the depth emission of ZnO nanostructures¹⁹.

To the best of our knowledge, the study of Al-Cu co-doped ZnO nanorods is still rare since last decade. Hence, to continue our previous work, in this paper we studied the influence of different Al-Cu compositions in ZnO nanorods. The Al composition was maintained lower than Cu to preserve lower solubility. In a further study, we performed the annealing post-treatment 500°C to reduce the native defects responsible for deep-level emission (DLE).

2. Experimental Methods

We have demonstrated the experiments as reported in the previous work¹. The ZnO seed layer was deposited on the top indium tin oxide (ITO) glass substrate by a commercial 1.7 MHz ultrasonic atomizer. The 0.02 mol of zinc acetate dihydrate ($C_4H_6O_4Zn \cdot 2H_2O$) was dissolved in 50 mL of deionized (DI) water. The substrate is then heated to 450 °C. An aerosol of the precursor solution was sprayed and injected onto the indium tin oxide (ITO) glass substrate by the ultrasonic nebulizer for 10 minutes.

The next step was the growth of ZnO nanostructure by chemical bath deposition (CBD). The growth solution of 0.1 M containing zinc nitrate tetrahydrate ($N_2O_6Zn \cdot 4H_2O$), aluminum nitrate nonahydrate ($Al(NO_3)_3 \cdot 9H_2O$) (1 wt%, 3 wt%, and 5 wt%), copper (II) Nitrate trihydrate ($Cu(NO_3)_2 \cdot 3H_2O$) (maintained constant at 20 wt%) and hexamethylenetetramine ($C_6H_{12}N_4$) was dissolved in DI water. Then, the solutions were stirred and heated at 60°C until transparent solutions were obtained. The ZnO-seeded ITO substrates were carefully dipped in growth solution and then heated in an oven at a temperature of 95°C for 2 hours. In the last step, all the samples are annealed at the temperature of 500°C in an atmosphere ambient for one hour.

To confirm the atomic composition of Al and Cu in the ZnO site, then we performed energy dispersive x-ray spectroscopy (EDS). It's confirmed the non-doped ZnO nanorods have Zn and O contents of 12.31at.% and 75.14at.%, respectively. Meanwhile, for the Al-Cu co-doped ZnO thin films with the Al-Cu composition of (Al 1wt.%+Cu 20wt.%), (Al 3 wt.%+Cu 20wt.%), (Al 5 wt.%+Cu 20wt.%) have the atomic percentages are (Al 0.17at.%+Cu 2.20at.%), (Al 0.45at.%+Cu 11.32at.%), (Al 0.11at.%+Cu 10.19at.%), respectively.

3. Results and Discussion

The structural properties of non-doped and Al-Cu co-doped ZnO nanostructures have been performed by X-ray diffraction (XRD) measurement with $CuK\alpha$ radiation. Figure 1 shows the XRD pattern of non-doped and Al-Cu co-doped ZnO nanostructures. It observes the hkl of non-doped ZnO nanorods have six planes which are (100), (002), (101), (102), (110), and (103). According to the International Centre for Diffraction Data (ICDD) number #98-007-6641, all the samples possess the polycrystalline hexagonal wurtzite structure. With the presence of Al-Cu co-dopants, there is a disorder of the crystal plane. It can be seen from the figure, the hkl planes of (Al 0.17at.%+Cu 2.20at.%) and (Al 0.45at.%+Cu 11.32at.%) co-doped ZnO nanostructures are (100), (002), (101), (110), and (103). Meanwhile, the hkl of (Al 0.11at.%+Cu 10.19at.%) co-doped ZnO nanostructure was observed in (002) and (101) planes. It means, the number of hkl of ZnO nanostructures decreases by increasing atomic percentages of Al-Cu co-doped. Hence, the crystallinity of the ZnO nanostructure decrease by Al-Cu incorporation. However, there is no other phase except from the ITO. Moreover, by calculating the texture coefficient²⁰, all the samples have the preferred growth orientation in the (002) plane. Further observations, the lattice parameters are affected by the presence of Al-Cu co-doped ZnO nanostructures. Furthermore, the crystallite size of ZnO nanostructures corresponding to the preferred growth orientation in the (002) plane has been calculated by using Scherer's equation^{21,22}. As seen in Table 1, the

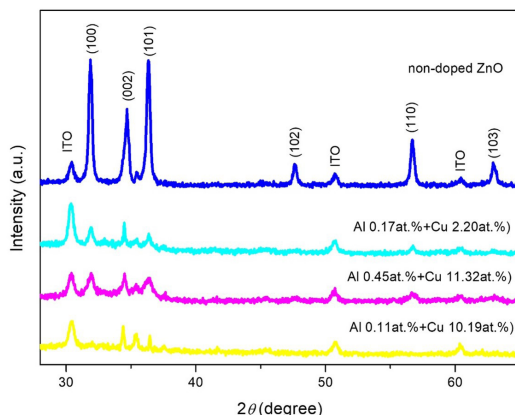
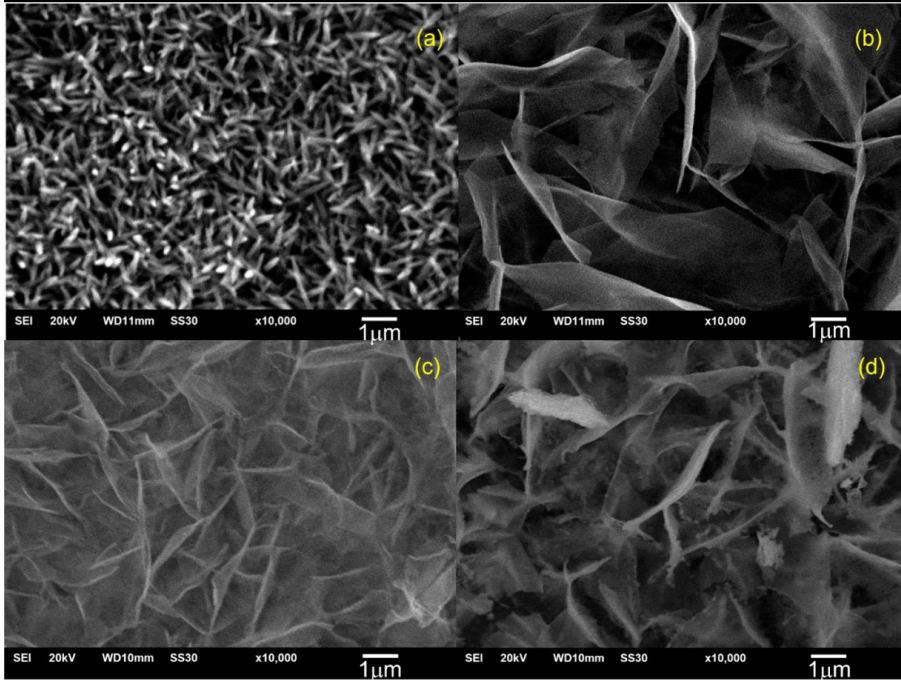


Figure 1. XRD pattern of non-doped and Al-Cu co-doped ZnO nanostructures.

Table 1. The structural parameters of non-doped and Al-Cu co-doped ZnO nanostructures calculated from the XRD pattern.

Sample	2θ ($^{\circ}$)	FWHM ($^{\circ}$)	a = b (\AA)	c (\AA)	c/a	Crystallite size (nm)
non-doped ZnO	34,68	0,4603	3,24	5,203	1,6	18,88
Al 0.17at.%+Cu 2.20at.%	34,47	0,1228	3,43	5,579	1,62	70,72
Al 0.45at.%+Cu 11.32at.%	34.50	0,2915	3,47	5,616	1,62	29,79
Al 0.11at.%+Cu 10.19at.%	34,39	0,1994	3,44	5,584	1,62	43,54

**Figure 2.** SEM images of non-doped and Al-Cu co-doped ZnO nanostructures, a) non-doped, b) Al 0.17at.%+Cu 2.20at.%, c) Al 0.45at.%+Cu 11.32at.%, d) Al 0.11at.%+Cu 10.19at.%.

crystallite size of ZnO nanostructures in the (002) plane of non-doped, (Al 0.17at.%+Cu 2.20at.%), (Al 0.45at.%+Cu 11.32at.%), and (Al 0.11at.%+Cu 10.19at.%) co-doped ZnO nanostructure are 18.88 nm, 70.72 nm, 29.79 nm, and 43.54 nm, respectively. It indicates the presence of Al-Cu as co-dopants tend to increase the value of lattice parameters which indicates the stress of the structure changed. As consequence, we confirmed the crystallite size of ZnO nanostructures increased with increasing Al-Cu content. On the other hand, others reported the incorporation of Al-Cu co-doped ZnO nanorods has smaller crystallite size compared to as-grown and Cu-doped ZnO nanorods⁴.

The morphology of the non-doped and Al-Cu co-doped ZnO nanostructures have been characterized by Scanning Electron Microscope (SEM) JEOL JSM-6510. Figure 2 shows the scanning electron microscope (SEM) images of non-doped and Al-Cu co-doped ZnO nanostructures. The morphology of the non-doped ZnO nanostructure confirmed that it has nanorod form. Post-annealing treatment did not influence the morphology of the ZnO nanorods (not shown here). However, the presence of Al-Cu co-dopant with different compositions strongly affects the morphology of ZnO nanostructures. It's

confirmed that more Cu dopants incorporated into the ZnO site will suppress the growth of ZnO nanostructures in the c-axis. According to our previous results, the Cu dopant suppresses the preferential growth along the c-axis and the Al dopant controls the growth in the other direction¹. Hence, we believed that the role of Cu in Al-Cu co doped ZnO nanostructures cause the morphology of nanostructure to change from nanorods to other forms i.e., nanodisks/nanosheets.

To observe the optical properties of non-doped and Al-Cu co-doped ZnO nanostructures, we have observed reflectance (R%) by UV-Vis Spectrophotometer (UV-Vis HITACHI U-3900H) at room temperature. The R% of non-doped and Al-Cu co-doped ZnO nanostructures at room temperature under atmosphere ambient are shown in Figure 3. It is seen that the reflectance of all the samples in the range of 300nm – 365nm is almost zero. Meanwhile, the reflectance of Al-Cu co-doped ZnO nanostructures in the range of 360 nm – 680 nm decrease by the increasing atomic percentage of Al and Cu.co-dopants. Hence, we believed that the reflectance is strongly influenced by the presence of Al-Cu atoms which modify the surface morphology of

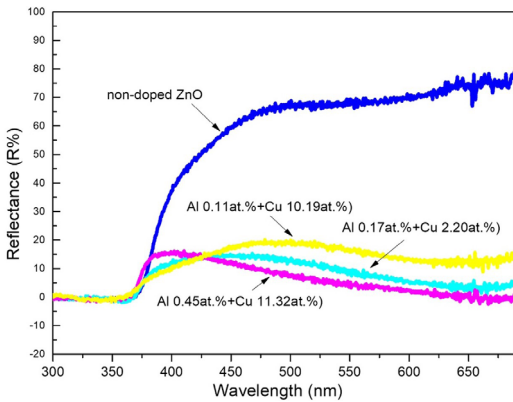


Figure 3. The reflectance spectra of non-doped and Al-Cu co-doped ZnO nanostructures at room temperature.

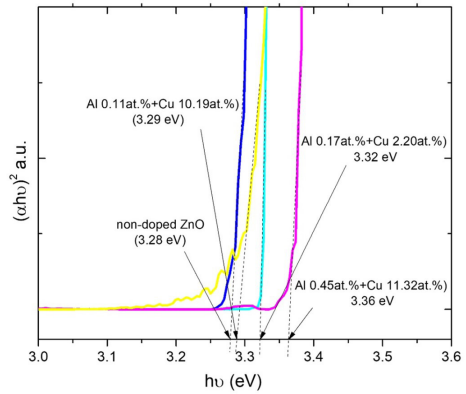


Figure 4. The optical band gap energy of non-doped and Al-Cu co-doped ZnO nanostructures.

the ZnO nanorods. Furthermore, according to the reflectance spectra we have estimated the optical band gap energy of ZnO nanostructures by using the Kubelka-Munk equation and Tauc-plot²³. Figure 4 shows the optical band gap energy of non-doped and Al-Cu co-doped ZnO nanostructures at room temperature. We observed the optical band gap energy of non-doped, (Al 0.17at.%+Cu 2.20at.%), (Al 0.45at.%+Cu 11.32at.%), and (Al 0.11at.%+Cu 10.19at.%) co-doped ZnO nanostructure is 3.28 eV, 3.32 eV, 3.36 eV, and 3.29 eV, respectively. It's seen that the ZnO nanostructures with Al and Cu compositions of 0.45at.% and 11.32at.%, respectively, have higher band gap energy of 3.36 eV. These Al-Cu dopants cause the incorporation of Al ions in the Zn site instead of Cu ions. Hence, the Burstein-Moss effect will cause the carrier concentration in the conduction band increased⁴. As results, there is blue shifting and the optical band gap energy of Al-Cu co-doped ZnO nanostructures tend to increase. Furthermore, the increase of the optical band gap energy is due to the presence of Cu in the ZnO site. It is relevant to our previous report that the band gap energy was dependent on the presence of Cu rather than Al¹. Moreover, Figure 5 depicts the correlation of crystallite size and band gap energy of non-doped and Al-Cu co-doped ZnO nanostructures. The crystallite size of ZnO nanostructures in the (002) plane tends to increase by the presence of Al-Cu co-doped (Table 1). Furthermore, as seen in Figure 5, the Al-Cu co-doped ZnO nanostructures with the content Al and Cu are 0.17at.% and 2.20at.%, respectively have band gap energy of 3.32 eV which are higher than the non-doped ZnO. Meanwhile, the crystallite size of Al 0.17at.%+Cu 2.20at.% co-doped ZnO nanostructures are higher than the other Al-Cu composition. To the best of our knowledge, the Burstein-Moss influences the value of band gap energy and affects the crystallite size of Al-Cu co-doped ZnO nanostructures. Qualitatively, our results indicate the role of Cu is more dominant than Al dopant which has lower solubility. It is confirmed by the increasing value of lattice parameters, band gap energy, and crystallite size. Cu ions which have a similar size to the Zn are most probable to be substituted in Zn site.

Furthermore, we investigated the optical photoluminescence (PL) properties of ZnO nanostructures using a femtosecond

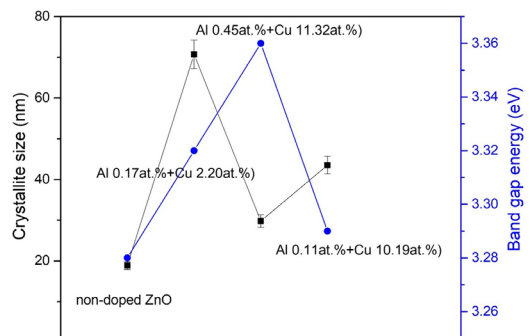


Figure 5. The band gap energy and crystallite size of non-doped and Al-Cu co-doped ZnO nanostructures in (002) plane.

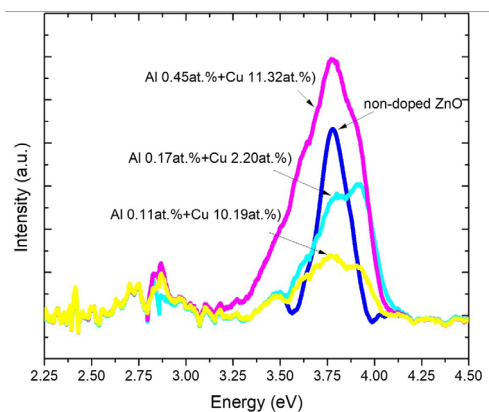


Figure 6. The PL spectra of non-doped and Al-Cu co-doped ZnO nanostructures at room temperature.

laser (at the excitation wavelength of 325 nm). As reported, the ZnO nanostructures have typical two peaks emissions which are near band edge (NBE) and deep level emission (DLE) emissions. These two typical emissions are due to the recombination of the free excitons and the native defects (i.e. oxygen vacancy (Vo), interstitial zinc (Zni), interstitial oxygen (Oi), and zinc vacancy (Vzn))²⁴. Figure 6 illustrates

the PL spectra of non-doped and Al-Cu co-doped ZnO nanostructures at room temperature under the atmosphere ambient. As seen in the figure, the PL spectra of non-doped and Al-Cu co-doped ZnO nanostructures have strong UV emission peaks at 3.78 eV (328 nm). However, for Al-Cu co-doped with the atomic percentage of (Al 0.17at.%+Cu 2.20at.%) and (Al 0.11at.%+Cu 10.19at.%), there is an additional peak at about 3.90 eV (318nm). Meanwhile, the Al-Cu co-doped ZnO with the atomic percentage of (Al 0.45at.%+Cu 11.32at.%) the additional peak is compensated by the intense peak 3.78 eV. The presence of Al-Cu co-doped ZnO nanostructures causes the existence of the complex spectra near the band edge due to the existence of increasing the carrier concentration in the conduction band. It's relevant to the Burstein-Moss effect which responsible to the increasing of band gap energy of Al-Cu co-doped ZnO nanostructures. As reported, the increasing carrier concentrations originated from the substitution of Zn by Cu ions¹¹. Furthermore, the complex spectra located near the band edge of the conduction band are caused by the presence of spin-orbit interaction and the exciton binding energy in the ZnO structure²⁵.

4. Conclusions

In conclusion, the morphology of the ZnO nanostructure is strongly affected by the presence of Al-Cu co-doped. Structurally, all samples possess polycrystalline hexagonal wurtzite structure, and the addition of Al-Cu decreases the crystallinity of ZnO nanostructures. Optically, the presence of Al-Cu co-doped affects the modification surface morphology of ZnO nanostructures, creates complex spectra near the band edge of ZnO band gap energy, and can be used to modify optical band gap energy. Hence, we recommend that the Al-Cu co-dopants modify the surface morphology and optical properties of ZnO nanostructures.

5. Acknowledgments

Financial support from Hibah Penelitian kompetitif Kolaborasi Internasional Universitas Negeri Jakarta Nomor No. 5/KI/LPPM/IV/2022 is gratefully acknowledged.

6. References

- Iwan S, Fauzia V, Azeti RA, Maharani ML, Fahdiran R, Budi E. Morphology and optical properties of Cu–Al co-doped ZnO nanostructures. *Surf Interfaces*. 2019;16:147-51. <http://dx.doi.org/10.1016/j.surf.2019.05.009>.
- Raha S, Ahmaruzzaman M. ZnO nanostructured materials and their potential applications: progress, challenges and perspectives. *Nanoscale Adv*. 2022;4:1868-925. <http://dx.doi.org/10.1039/d1na00880c>.
- Hang DR, Islam SE, Sharma KH, Kuo SW, Zhang CZ, Wang JJ. Annealing effects on the optical and morphological properties of ZnO nanorods on AZO substrate by using aqueous solution method at low temperature. *Nanoscale Res Lett*. 2014;9:1-7. <http://dx.doi.org/10.1186/1556-276X-9-632>.
- Chakraborty M, Mahapatra P, Thangavel R. Structural, optical and electrochemical properties of Al and Cu co-doped ZnO nanorods synthesized by a hydrothermal method. *Thin Solid Films*. 2016;612:49-54. <http://dx.doi.org/10.1016/j.tsf.2016.05.038>.
- Iwan S, Zhao JL, Tan ST, Sun XW. Enhancement of UV photoluminescence in ZnO tubes grown by metal organic chemical vapour deposition (MOCVD). *Vacuum*. 2018;155:408-11. <http://dx.doi.org/10.1016/j.vacuum.2018.06.035>.
- Huang ZL, Chen CM, Lin ZK, Yang SH. Efficiency enhancement of regular-type perovskite solar cells based on Al-doped ZnO nanorods as electron transporting layers. *Superlattices Microstruct*. 2017;102:94-102. <http://dx.doi.org/10.1016/j.spmi.2016.12.012>.
- Kishwar S, Ul Hasan K, Alvi NH, Klason P, Nur O, Willander M. A comparative study of the electrodeposition and the aqueous chemical growth techniques for the utilization of ZnO nanorods on p-GaN for white light emitting diodes. *Superlattices Microstruct*. 2011;49:32-42. <http://dx.doi.org/10.1016/j.spmi.2010.10.004>.
- Wang ZL. Zinc oxide nanostructures: growth, properties and applications. *J Phys Condens Matter*. 2004;16:829-58. <http://dx.doi.org/10.1088/0953-8984/16/25/R01>.
- Roza L, Febrianti Y, Iwan S, Fauzia V. The role of cobalt doping on the photocatalytic activity enhancement of ZnO nanorods under UV light irradiation. *Surf Interfaces*. 2020;18:100435. <http://dx.doi.org/10.1016/j.surf.2020.100435>.
- Zhang Y, Yang Z, Tang L, Shen Y, Wu Y, Zhang N et al. UV luminescence enhancement of Cu-doped ZnO nanorods grown by hydrothermal treatment. *J Lumin*. 2022;252:119364. <http://dx.doi.org/10.1016/j.jlumin.2022.119364>.
- Alev O, Ergün İ, Özdemir O, Arslan LÇ, Büyükköse S, Öztürk ZZ. Enhanced ethanol sensing performance of Cu-doped ZnO nanorods. *Mater Sci Semicond Process*. 2021;136:106149. <http://dx.doi.org/10.1016/j.mssp.2021.106149>.
- Bu IYY. Sol-gel production of Cu/Al co-doped zinc oxide: effect of Al co-doping concentration on its structure and optoelectronic properties. *Superlattices Microstruct*. 2014;76:115-24. <http://dx.doi.org/10.1016/j.spmi.2014.09.011>.
- Islam MR, Rahman M, Farhad SFU, Podder J. Structural, optical and photocatalysis properties of sol-gel deposited Al-doped ZnO thin films. *Surf Interfaces*. 2019;16:120-6. <http://dx.doi.org/10.1016/j.surf.2019.05.007>.
- Yang J, Liu X, Yang L, Wang Y, Zhang Y, Lang J et al. Effect of annealing temperature on the structure and optical properties of ZnO nanoparticles. *J Alloys Compd*. 2009;477:632-5. <http://dx.doi.org/10.1016/j.jallcom.2008.10.135>.
- Narayanan GN, Ganesh RS, Karthigeyan A. Effect of annealing temperature on structural, optical and electrical properties of hydrothermal assisted zinc oxide nanorods. *Thin Solid Films*. 2016;598:39-45. <http://dx.doi.org/10.1016/j.tsf.2015.11.071>.
- Umar A, Kumar R, Kumar G, Algarni H, Kim SH. Effect of annealing temperature on the properties and photocatalytic efficiencies of ZnO nanoparticles. *J Alloys Compd*. 2015;648:46-52. <http://dx.doi.org/10.1016/j.jallcom.2015.04.236>.
- Barnett CJ, Mourgelas V, McGettrick JD, Maffei TGG, Barron AR, Cobley RJ. The effects of vacuum annealing on the conduction characteristics of ZnO nanorods. *Mater Lett*. 2019;243:144-7. <http://dx.doi.org/10.1016/j.matlet.2019.02.005>.
- Sushama S, Murkute P, Ghadi H, Pandey SK, Chakrabarti S. Enhancement in structural, elemental and optical properties of boron-phosphorus Co-doped ZnO thin films by high-temperature annealing. *J Lumin*. 2021;238:118221. <http://dx.doi.org/10.1016/j.jlumin.2021.118221>.
- Iwan S, Fauzia V, Umar AA, Sun XW. Room temperature photoluminescence properties of ZnO nanorods grown by hydrothermal reaction. *AIP Conf Proc*. 2016;1729:020031. <http://dx.doi.org/10.1063/1.4946934>.
- Caglar Y, Ilican S, Caglar M, Yakuphanoglu F, Wu J, Gao K et al. Influence of heat treatment on the nanocrystalline structure of ZnO film deposited on p-Si. *J Alloys Compd*. 2009;481:885-9. <http://dx.doi.org/10.1016/j.jallcom.2009.03.140>.
- Pushpa N, Kokila MK. Effect of cobalt doping on structural, thermo and photoluminescent properties of ZnO nanopowders. *J Lumin*. 2017;190:100-7. <http://dx.doi.org/10.1016/j.jlumin.2017.05.032>.

22. Sugihartono I, Silmina AD, Fahdiran R, Isnaeni I. The effects of substrate on enhancement of UV emission of ZnO nanorods. *J Phys Conf Ser.* 2019;1402:066008. <https://doi.org/10.1088/1742-6596/1402/6/066008>.
23. Mohar RS, Sugihartono I, Fauzia V, Umar AA. Dependence of optical properties of Mg-doped ZnO nanorods on Al dopant. *Surf Interfaces.* 2020;19:100518. <http://dx.doi.org/10.1016/j.surfin.2020.100518>.
24. Fan XM, Lian JS, Guo ZX, Lu HJ. Microstructure and photoluminescence properties of ZnO thin films grown by PLD on Si(1 1 1) substrates. *Appl Surf Sci.* 2005;239:176-81. <http://dx.doi.org/10.1016/j.apsusc.2004.05.144>.
25. Özgür Ü, Alivov YI, Liu C, Teke A, Reshchikov MA, Doğan S et al. A comprehensive review of ZnO materials and devices. *J Appl Phys.* 2005;98:041301. <http://dx.doi.org/10.1063/1.1992666>.